Journal of Sound and Vibration (2000) **238**(1), 85–111
doi:10.1006/jsvi.2000.3080, available online at http://www.idealibrary.com on IDEAL®

INFLUENCES OF SMALL CURVATURES ON THE MODAL CHARACTERISTICS OF THE JOINED HERMETIC SHELL STRUCTURES

D. T. HUANG

Department of Mechanical Engineering, Nan-Kai College of Technology, Tsao-Twen, Nan-Tou, Taiwan, 542, Republic of China. E-mail: tyhuang@bear.nkjc.edu.tw

(*Received* 14 *June* 1999, *and in final form* 12 *May* 2000)

From a practical engineering point of view, there is interest in understanding the influences of small curvatures on the modal characteristics of a plate–shell combination. However, research reports in this area are rarely found in literature. This paper is the first one to study the influences of small curvatures on free vibration of a plate–shell combined structure, consisting of a circular barrel-like shell and two spherically curved end plates, using the line receptance concepts and approximate frequency equations of barrel-shaped shell and spherically curved plate. It illustrates in detail information about natural frequencies and mode shapes of the combined structure under different geometric configurations. Consequently, it provides useful information for setting up criteria for designing hermetic plate-shell joined structures, such as the hermetic shell of a refrigeration compressor. The receptance method, which is basically a component mode synthesis technique, is adopted as the solution procedure in this study. It predicts the responses and frequencies of a combined system in terms of the responses and frequencies of its subsystems. This technique, for cases to which it can be applied successfully, is a powerful tool in creating an understanding of the physics of combined structures.

1. INTRODUCTION

When a shell of revolution (cylindrical, spherical, conical, etc.) is coupled with end or intermediate plates (flat or spherically curved), the dynamic behavior of the combined structure becomes relatively complicated. The wide engineering applications of these joined structures in different areas, such as pressure vessels, refrigeration compressors, nuclear reactors, ships, submarines, aeronautical and space structures, have attracted considerable research interest and promoted development of different methods for analyzing their vibration characteristics.

Computer programs, mostly based on the finite element method, were used to obtain the natural frequencies and modes of plate–shell combined structures with any combination of boundary conditions with an accuracy sufficient for most engineering applications. However, the natural frequencies and corresponding mode shapes obtained by the finite element method are mixtures of three categories, namely, the axial mode, the tangential mode and the transverse mode. Comparing with numerical approaches such as the finite element method, analytical approaches are often appropriate in playing the role of providing physical insight into the vibration characteristics of the combined structure. The vibration modes in a specific category can be obtained in the order of natural frequency by analytical approaches without bringing modes belonging to other categories.

0022-460X/00/460085 + 27 $35.00/0

Researchers have applied analytical approaches for modal analysis of the combined structures for a long time. Smith and Haft [1, 2] used the classical method of matching all the boundary conditions at the intersection of a circular cylindrical shell and an elastic plate to determine the natural frequencies and mode shapes. Hirano [3], and Takahashi and Hirano [4, 5] studied the free vibrations of vessels consisting of thin-walled cylindrical shells and circular plates, by formulating the Lagrangian of the combined system in the form of the unknown boundary values of displacement and slope. Using the conditions of continuity, the frequencies and the displacements were determined by means of minimizing the total Lagrangian with respect to the unknown boundary values. Suzuki *et al.* [6, 7] investigated the free vibration of thick-walled vessels with variable thickness by incorporating thick plate and shell theories. Kosawada *et al.* [8] analyzed the asymmetric vibration of a combined system consisting of a barrel-like shell of revolution having constant meridional curvature and circular plate lids. Suzuki *et al.* [9] studied the free vibrations of a vessel consisting of circular plates and a shell of revolution with varying meridional curvature. The same solution technique used in references [3–5] was applied in references [6–9]. Irie *et al.* [10, 11] applied the transfer matrix method to study free vibration of joined shells. Yamada *et al.* [12] studied the free vibration of a circular cylindrical double-shell system closed by end plates. Tavakoli and Singh [13–15] proposed a state-space method, which is a transfer matrix-based substructuring technique, for modal analysis of a hermetic can with a circular cylindrical shell and two circular end plates. Cheng and Nicolas [16] used the variational approach and incorporated extensional and torsional springs with spring constants adjustable to simulate the boundary conditions and coupling conditions at the interface of a circular cylindrical shell and a circular plate for vibration analysis. The method of matching mechanical impedances for the subsystems has also been applied. Sakarov [17] introduced the method of dynamic rigidities, which are related to impedances, for joined systems along a line and applied it to a circular cylindrical shell with an annular plate at one end. Faulkner [18], Wilken and Soedel [19, 20], and Azimi *et al.* [21–24] applied the concept of line receptances to combinations of shells, rings and plates. Huang and Soedel [25–27] further implemented the receptance method to study the effects of changes in geometry and joining position on vibrational behavior of a multiple plates–shell combination, explore structural coupling behavior between the shell and the plate, and investigate forced vibration and vibration cancellation of the plate–shell combinations. Lately, Wong and Sze [28] applied matched asymptotic expansion method and used membrane approximation to analyze the torsion–free axi-symmetric vibration modes of thin cylindrical shell with hemispherical caps.

Properly applied these analytical approaches can effectively solve eigenvalue problems of certain structural configurations and obtain some vibration characteristics. From a practical engineering point of view, there is interest in understanding the influences of small curvatures on the modal characteristics of plate–shell combination. However, research reports in this area, such as the one published by Wong and Sze [28], are rarely found in literature. This paper is the first one to study the influences of small curvatures on the free vibration of a plate–shell combined structure, consisting of a circular barrel-like shell and two spherically curved end plates, using the line receptance concepts and approximate frequency equations of barrel-shaped shell and spherically curved plate. It illustrates in detail information about natural frequencies and mode shapes of the combined structure under different geometric configurations. Consequently, it provides useful information for setting up criteria for designing hermetic plate–shell joined structures, such as the hermetic shell of a refrigeration compressor.

The receptance method, which is basically a component mode synthesis technique, is adopted as the solution procedure in this study. It predicts the responses and frequencies of

a combined system in terms of the responses and frequencies of its subsystems. This technique, for cases to which it can be applied successfully, is a powerful tool in creating an understanding of the physics of combined structures. An advantage of using the receptance method is that the receptances of the subsystems may be determined by any method, which is sufficiently accurate. Thus, they can be obtained analytically, experimentally, or numerically.

2. SYSTEM RECEPTANCES

Bishop and Johnson [29] defined a receptance as the ratio of a displacement or slope response at a certain point to a harmonic force or moment input at the same or a different point. When structures are joined along lines, line receptances may be defined and treated the same as point receptances under the condition that the spatial dependencies of the receptance can be eliminated. This condition is usually satisfied if shells of revolution are joined to other shells of revolution along the joint circles or to structures of revolution such as circular rings or plates. For the case where two circular plates are joined to a circular cylindrical shell, in general, five displacement or slope connections and five force or moment connections could be considered for each plate–shell pair. The possibilities are displacements in three directions and slopes in two directions (consistent with the classical thin shell theory) for the shell and corresponding displacements or slopes of the plate, together with appropriate force or moment connections. The force or moment connections are line loads, which vary with $\sin n\theta$ or $\cos n\theta$, on the argument that at each natural frequency of the joined system; the associated mode shape component varies with $\sin n\theta$ or $\cos n\theta$ in circumferential direction. Thus, the connecting forces or moments must vary with $\sin n\theta$ or $\cos n\theta$. It is assumed that the plate and the shell are joined at the reference surfaces.

The full treatment of using five connections is not necessary, if one limits the analysis to the lower frequencies and modes of the system. For these modes, it is reasonable to assume that the circular plate is inelastic in its plane and admits only transverse deflections and a rigid-body motion in its plane. Also, compared to typical expected transverse amplitudes of the connected system, possible influences of small connection deflections in the tangential planes of the shell can be neglected. The number of connections of each plate–shell joint pair can be reduced to two, namely the radial slope changes at the plate boundary coupled to axial slope changes of the shell and the radial rigid-body motion of the plate coupled to a transverse motion of the shell. A similar approach was used by Sakarov [17] and Faulkner [18], respectively, except that only one connection was needed there since the plates were attached to the shell at the shell's simple supports, which suppress the rigid-body modes of the plate.

The displacement (or slope) amplitudes X_{Ai} ($i = 1$–10), as functions of harmonic force (or moment) amplitudes F_{Aj} ($j = 1$–10), are

$$\{X_{Ai}\} = [\alpha_{ij}]^{\mathrm{T}}\{F_{Aj}\}, \tag{1}$$

where α_{ij} are the receptances of system A. Similarly,

$$\{X_{Bp}\} = [\beta_{pq}]^{\mathrm{T}}\{F_{Bq}\}, \tag{2}$$

where β_{pq} ($p = 1$–5 and $q = 1$–5) are the receptances of system B. Also,

$$\{X_{Cs}\} = [\gamma_{st}]^{\mathrm{T}}\{F_{Ct}\}, \tag{3}$$

where γ_{st} ($s = 6$–10 and $t = 6$–10) are the receptances of system C.

When the three systems are joined and no forces (or moments) external to the three systems are applied, it must be that $\{F_{Bq}\} = -\{F_{Aq}\}$ and $\{F_{Ct}\} = -\{F_{At}\}$. Also, due to displacement (or slope) continuity, it must be that $\{X_{Bp}\} = \{X_{Ap}\}$ and $\{X_{Cs}\} = \{X_{As}\}$.

Suitably combining equations (1)–(3) and applying the above equalities gives

$$\begin{bmatrix} \alpha_{pq} + \beta_{pq} & \alpha_{pt} \\ \alpha_{sq} & \alpha_{st} + \gamma_{st} \end{bmatrix} \begin{Bmatrix} F_{Bq} \\ F_{Ct} \end{Bmatrix} = 0. \tag{4}$$

For the simplification employed here, equation (4) reduces to

$$\begin{bmatrix} \alpha_{11} + \beta_{11} & \alpha_{12} + \beta_{12} & \alpha_{13} & \alpha_{14} \\ \alpha_{21} + \beta_{21} & \alpha_{22} + \beta_{22} & \alpha_{23} & \alpha_{24} \\ \alpha_{31} & \alpha_{32} & \alpha_{33} + \gamma_{33} & \alpha_{34} + \gamma_{34} \\ \alpha_{41} & \alpha_{42} & \alpha_{43} + \gamma_{43} & \alpha_{44} + \gamma_{44} \end{bmatrix} \begin{Bmatrix} F_1 \\ M_1 \\ F_2 \\ M_2 \end{Bmatrix} = 0. \tag{5}$$

where F is the amplitude of the force which couples the rigid planar motion of the plate to the motion of the shell and M is the amplitude of the moment which couples the transverse motion of the plate to the motion of the shell. The subscripts 1 and 2 indicate the first and the second plate–shell joint pairs respectively. The receptances β_{12}, β_{21}, γ_{34} and γ_{43} are zero due to zero coupling of transverse plate motion to in-plane plate motion. The system frequency equation of a two plates–shell combination reduces to

$$\begin{bmatrix} \alpha_{11} + \beta_{11} & \alpha_{12} & \alpha_{13} & \alpha_{14} \\ \alpha_{21} & \alpha_{22} + \beta_{22} & \alpha_{23} & \alpha_{24} \\ \alpha_{31} & \alpha_{32} & \alpha_{33} + \gamma_{33} & \alpha_{34} \\ \alpha_{41} & \alpha_{42} & \alpha_{43} & \alpha_{44} + \gamma_{44} \end{bmatrix} = 0. \tag{6}$$

3. FORMULATION OF RECEPTANCES

3.1. SHELL RECEPTANCES

For the case that one circular plate is joined to a circular cylindrical shell. The transverse deflection, $u_3(x^*, \theta, t)$, is caused by the transverse loading, so is the slope of the axial direction, $\beta_x(x^*, \theta, t)$. They are required for formulating the receptance due to the displacement response of the shell at x^* to line force loading at x^*, α_{11}, and the receptance due to the slope response of the shell at x^* to line force loading at x^*, α_{21}. These receptances are defined as

$$\alpha_{11} = \frac{u_3(x^*, \theta, t)}{F_3(x^*, \theta, t)}, \tag{7}$$

$$\alpha_{21} = \frac{\beta_r(x^*, \theta, t)}{F_3(x^*, \theta, t)}. \tag{8}$$

To obtain these receptances, one has to solve the problem of a shell loaded by a transverse line forcing $F_3(x, \theta, t)$,

$$F_3(x, \theta, t) = F_0 \cos P\theta \delta(x - x^*) e^{j\omega t}, \tag{9}$$

where 3 denotes the transverse direction, F_0 is the amplitude of the line load which couples the rigid planar motion of the plate to the motion of shell, $P = 0, 1, 2, \ldots, \delta(x - x^*)$ is a Dirac-delta function, and x^* is the location of the line load. The equations of the natural modes of a simply supported cylindrical shell, including the longitudinal mode, the circumferential mode and the transverse mode, are expressed as

$$U^s_{xkmn}(x, \theta) = (A_{kmn}/C_{kmn}) \cos(m\pi x/L_s) \cos n(\theta - \phi),$$

$$U^s_{\theta kmn}(x, \theta) = (B_{kmn}/C_{kmn}) \sin(m\pi x/L_s) \sin n(\theta - \phi), \tag{10}$$

$$U^s_{3kmn}(x, \theta) = \sin(m\pi x/L_s) \cos n(\theta - \phi),$$

where $m = 1, 2, \ldots, n = 0, 1, 2, \ldots, k = 1, 2, 3$, and $\theta = 0, \pi/2n$. The mode amplitude ratios (A_{kmn}/C_{kmn}) and (B_{kmn}/C_{kmn}) are discussed by Soedel [30] and given in Appendix A.

The transverse deflection due to line force loading is of the form

$$u_3(x, \theta, t) = \sum_{k=1}^{3} \sum_{m=1}^{\infty} \frac{2F_0 \sin(m\pi x^*/L_s) \sin(m\pi x/L_s) \cos n\theta \, e^{j\omega t}}{\rho h_s L_s [(A_{kmn}/C_{kmn})^2 + (B_{kmn}/C_{kmn})^2 + 1](\omega^2_{kmn} - \omega^2)}, \tag{11}$$

where $n = P$. Note that the summation over n has been eliminated because of the orthogonality of the forcing function component $\cos P\theta$ with the mode component $\cos n\theta$. Also, $\phi = 0$ was used for this derivation since the non-preferential direction of the modes for a system of revolution does not enter the receptance formulation. The $\phi = \pi/2n$ modes have the same natural frequencies and mode shapes, but shifted by ϕ in the θ direction. The natural frequencies of a simply supported cylindrical shell, ω_{kmn}, $k = 1, 2, 3$, corresponding to the transverse mode, the longitudinal mode and the circumferential mode, respectively, are also given in Appendix A.

The slope response due to line force loading is obtained by differentiating equation (11):

$$\beta_x = -\frac{\partial u_3}{\partial x} = \sum_{k=1}^{3} \sum_{m=1}^{\infty} \frac{-2F_0 m\pi \sin(m\pi x^*/L_s) \cos(m\pi x/L_s) \cos n\theta \, e^{j\omega t}}{\rho h_s L_s^2 [(A_{kmn}/C_{kmn})^2 + (B_{kmn}/C_{kmn})^2 + 1](\omega^2_{kmn} - \omega^2)}, \tag{12}$$

Evaluating equations (11) and (12) at $x = x^*$ and dividing them by equation (9) gives

$$\alpha_{11} = \sum_{k=1}^{3} \sum_{m=1}^{\infty} \frac{2 \sin^2(m\pi x^*/L_s)}{\rho h_s L_s [(A_{kmn}/C_{kmn})^2 + (B_{kmn}/C_{kmn})^2 + 1](\omega^2_{kmn} - \omega^2)}, \tag{13}$$

$$\alpha_{21} = \sum_{k=1}^{3} \sum_{m=1}^{\infty} \frac{-2m\pi \sin(m\pi x^*/L_s) \cos(m\pi x^*/L_s)}{\rho h_s L_s^2 [(A_{kmn}/C_{kmn})^2 + (B_{kmn}/C_{kmn})^2 + 1](\omega^2_{kmn} - \omega^2)}, \tag{14}$$

The receptance due to the slope response of the shell at x^* to line moment loading at x^* is denoted as α_{22}. While the receptance due to the displacement response of the shell at x^* to line moment loading at x^* is denoted as α_{12}. These two receptances are defined as

$$\alpha_{22} = \frac{\beta_x(x^*, \theta, t)}{M_x(x^*, \theta, t)}, \tag{15}$$

$$\alpha_{12} = \frac{u_3(x^*, \theta, t)}{M_x(x^*, \theta, t)}. \tag{16}$$

To obtain these receptances, one has to solve the problem of a shell excited by a line moment

$$M_x(x, \theta, t) = M_0 \cos P\theta \delta(x - x^*) e^{j\omega t}, \tag{17}$$

where $M_x(x, \theta, t)$ is a distributed moment and M_0 is the amplitude of the moment per unit length in circumferential direction. The displacement response of the shell due to line moment loading is of the form

$$u_3(x, \theta, t) = -\sum_{k=1}^{3} \sum_{m=1}^{\infty} \frac{2M_0 \pi m \cos(m\pi x^*/L_s) \sin(m\pi x/L_s) \cos n\theta \, e^{j\omega t}}{\rho h_s L_s^2 [(A_{kmn}/C_{kmn})^2 + (B_{kmn}/C_{kmn})^2 + 1](\omega_{kmn}^2 - \omega^2)}. \tag{18}$$

The slope response of the shell due to line moment loading is again obtained by differentiation

$$\beta_x(x, \theta, t) = \sum_{k=1}^{3} \sum_{m=1}^{\infty} \frac{2M_0 m^2 \pi^2 \cos(m\pi x^*/L_s) \cos(m\pi x/L_s) \cos n\theta \, e^{j\omega t}}{\rho h_s L_s^3 [(A_{kmn}/C_{kmn})^2 + (B_{kmn}/C_{kmn})^2 + 1](\omega_{kmn}^2 - \omega^2)}. \tag{19}$$

Evaluating equations (18) and (19) at $x = x^*$ and dividing them by equation (17), equations (15) and (16) become

$$\alpha_{22} = \sum_{k=1}^{3} \sum_{m=1}^{\infty} \frac{2(m\pi)^2 \cos^2(m\pi x^*/L_s)}{\rho h_s L_s^3 [(A_{kmn}/C_{kmn})^2 + (B_{kmn}/C_{kmn})^2 + 1](\omega_{kmn}^2 - \omega^2)}. \tag{20}$$

$$\alpha_{12} = \sum_{k=1}^{3} \sum_{m=1}^{\infty} \frac{-2m\pi \sin(m\pi x^*/L_s) \cos(m\pi x^*/L_s)}{\rho h_s L_s^2 [(A_{kmn}/C_{kmn})^2 + (B_{kmn}/C_{kmn})^2 + 1](\omega_{kmn}^2 - \omega^2)}. \tag{21}$$

When two circular plates are joined to the shell, the coupling harmonic line forces and line moments are

$$F_{3i}(x, \theta, t) = F_{0i} \cos P\theta \delta(x - x_i^*) e^{j\omega t}, \tag{22}$$

and

$$M_{xi}(x, \theta, t) = M_{0i} \cos P\theta \delta(x - x_i^*) e^{j\omega t}, \tag{23}$$

where F_{0i}, M_{0i} $(i = 1, 2)$ are the magnitudes of the coupling line forces and line moments between the plates and the shell, $P = 0, 1, 2, \ldots, \delta(x - x_1^*)$ is the Dirac-delta function, and x_i^* $(i = 1, 2)$ are the locations where the plates are joined to the shell. Using the same approach in deriving the shell receptances for the single plate–shell case, the receptances of the shell, which is connected by two circular plates, can be defined as:

(1) The receptance due to the displacement response of the shell at $x_i^* (i = 1, 2)$ to the coupling line force at $x_j^* (j = 1,2)$ is

$$\alpha_{bd} = \sum_{k=1}^{3} \sum_{m=1}^{\infty} \frac{2 \sin(m\pi x_i^*/L_s) \sin(m\pi x_j^*/L_s)}{\rho h_s L_s [(A_{kmn}/C_{kmn})^2 + (B_{kmn}/C_{kmn})^2 + 1](\omega_{kmn}^2 - \omega^2)}, \tag{24}$$

where $b = 2i - 1$ and $d = 2j - 1$.

(2) The receptance due to the displacement response of the shell at $x_i^*(i = 1, 2)$ to the coupling line moment at $x_j^*(j = 1,2)$ is

$$\alpha_{bg} = \sum_{k=1}^{3} \sum_{m=1}^{\infty} \frac{-2m\pi \sin(m\pi x_i^*/L_s) \sin(m\pi x_j^*/L_s)}{\rho h_s L_s^2 [(A_{kmn}/C_{kmn})^2 + (B_{kmn}/C_{kmn})^2 + 1](\omega_{kmn}^2 - \omega^2)}, \tag{25}$$

where $b = 2i - 1$ and $g = 2j$.

(3) The receptance due to the slope response of the shell at $x_i^*(i = 1, 2)$ to the coupling line force at $x_j^*(j = 1,2)$ is

$$\alpha_{fd} = \sum_{k=1}^{3} \sum_{m=1}^{\infty} \frac{-2m\pi \cos(m\pi x_i^*/L_s) \sin(m\pi x_j^*/L_s)}{\rho h_s L_s^2 [(A_{kmn}/C_{kmn})^2 + (B_{kmn}/C_{kmn})^2 + 1](\omega_{kmn}^2 - \omega^2)}, \tag{26}$$

where $f = 2i$ and $d = 2j - 1$.

(4) The receptance due to the slope response of the shell at $x_i^*(i = 1, 2)$ to the coupling line moment at $x_j^*(j = 1,2)$ is

$$\alpha_{fg} = \sum_{k=1}^{3} \sum_{m=1}^{\infty} \frac{2(m\pi)^2 \cos(m\pi x_i^*/L_s) \cos(m\pi x_j^*/L_s)}{\rho h_s L_s^3 [(A_{kmn}/C_{kmn})^2 + (B_{kmn}/C_{kmn})^2 + 1](\omega_{kmn}^2 - \omega^2)}, \tag{27}$$

where $f = 2i$ and $g = 2j$.

Comparing these 16 shell receptances, it is seen that $\alpha_{12} = \alpha_{21}$, $\alpha_{13} = \alpha_{31}$, $\alpha_{14} = \alpha_{41}$, $\alpha_{32} = \alpha_{23}$, $\alpha_{42} = \alpha_{24}$ and $\alpha_{43} = \alpha_{34}$, which is as expected from the reciprocity theorem.

3.2. PLATE RECEPTANCES

The radial deflection of a circular plate, which moves as a rigid body, is defined as $u_r(r, \theta, t)$; while the distributed force, which couples the plate to the shell, is defined as $F_r(r, \theta, t)$. In order to obtain the plate receptance

$$\beta_{11} = \frac{u_r(a, \theta, t)}{F_r(a, \theta, t)} \tag{28}$$

at the joint of the plate and the shell, where $r = a$, a tangential load

$$F_r(r, \theta, t) = F_0 \cos P\theta \, \delta(r - a) e^{j\omega t} \tag{29}$$

is applied on the plate. But because the plate can be viewed as inelastic in its in-plane motion (its lowest natural frequency due to elastic in-plane motion exceeds, for the typical cases of interest, the transverse frequencies by far), it can be treated as having rigid-body motion only. Therefore,

$$u_r(a, \theta, t) = U_0 \cos\theta e^{j\omega t}, \tag{30}$$

and the equation of motion reduces to

$$M\ddot{U}_r = \int_0^a \int_0^{2\pi} F_0 \cos P\theta \cos\theta \, e^{j\omega t} \delta(r - a) r \, dr \, d\theta, \tag{31}$$

where $M = \pi a^2 \rho h_p$ is the mass of the plate. Evaluating the equation results in

$$u_r(a, \theta, t) = \begin{cases} -a\pi F_0 \cos P\theta \mathrm{e}^{\mathrm{j}\omega t}/(M\omega^2), & P = 1, \\ 0, & P \neq 1. \end{cases} \tag{32}$$

Dividing equation (32) by equation (29), equation (28) becomes

$$\beta_{11} = \begin{cases} -1/(a\rho h_p \omega^2), & P = 1, \\ 0, & P \neq 1. \end{cases} \tag{33}$$

To obtain the receptance

$$\beta_{22} = \frac{\beta_r(a, \theta, t)}{M_r(a, \theta, t)}, \tag{34}$$

where $\beta_r(a, \theta, t)$ is the slope due to the moment loading, a line moment load is applied on the circular plate at $r = a$

$$M_r(r, \theta, t) = -M_0 \cos P\theta \delta(r - a) \mathrm{e}^{\mathrm{j}\omega t}. \tag{35}$$

The solution for the transverse deflection is of the form

$$u_3(r, \theta, t) = \sum_{m=1}^{\infty} \frac{F^*_{mn} U^p_{3mn}(r, \theta) \mathrm{e}^{\mathrm{j}\omega t}}{\omega^2_{mn} - \omega^2}, \tag{36}$$

where

$$U^p_{3mn}(r, \theta) = [\mathrm{J}_n(\lambda_{mn} r) - (\mathrm{J}_n(\lambda_{mn} a)/\mathrm{I}_n(\lambda_{mn} a))\mathrm{I}_n(\lambda_{mn} r)] \cos n(\theta - \phi), \tag{37}$$

$$\omega_{mn} = \frac{(\lambda_{mn} a)^2}{a^2} h_p \sqrt{\frac{E}{12(1 - \upsilon)\rho}}, \tag{38}$$

$$F^*_{mn} = \frac{-M_0 \pi \lambda_{mn} a}{\rho h N^p_{mn}} [\mathrm{J}_{n+1}(\lambda_{mn} a) - (\mathrm{J}_n(\lambda_{mn} a)/\mathrm{I}_n(\lambda_{mn} a)) I_{n+1}(\lambda_{mn} a)], \tag{39}$$

are the mode shape equation, the natural frequency equation and the magnitude of the coupling forcing function respectively. The plate modal mass is

$$N^p_{mn} = \pi \int_0^a [\mathrm{J}_n(\lambda_{mn} r) - \mathrm{J}_n(\lambda_{mn} a)\mathrm{I}_n(\lambda_{mn} r)/\mathrm{I}_n(\lambda_{mn} a)\}^2 r \, \mathrm{d}r. \tag{40}$$

The slope $\beta_r(r, \theta, t)$ is obtained by differentiation

$$\beta_r(r, \theta, t) = -\frac{\partial u_3(r, \theta, t)}{\partial r} = -\sum_{m=1}^{\infty} \frac{F^*_{mn} U^{p'}_{3mn}(r, \theta) \mathrm{e}^{\mathrm{j}\omega t}}{\omega^2_{mn} - \omega^2}, \tag{41}$$

where

$$U^{p'}_{3mn}(r, \theta) = \lambda_{mn} \{(n/\lambda_{mn} r)\mathrm{J}_n(\lambda_{mn} r) - \mathrm{J}_{n+1}(\lambda_{mn} r) - (\mathrm{J}_n(\lambda_{mn} a)/\mathrm{I}_n(\lambda_{mn} a))$$
$$[(n/\lambda_{mn} r)\mathrm{I}_n(\lambda_{mn} r) - \mathrm{I}_{n+1}(\lambda_{mn} r)]\} \cos n\theta. \tag{42}$$

Evaluating equation (41) at $r = a$, and dividing by equation (35), equation (34) becomes

$$\beta_{22} = \sum_{m=1}^{\infty} \frac{\pi\lambda_{mn}^2 a[\mathrm{J}_{n+1}(\lambda_{mn}a) - \mathrm{J}_n(\lambda_{mn}a)\mathrm{I}_{n+1}(\lambda_{mn}a)/\mathrm{I}_n(\lambda_{mn}a)]^2}{\rho h N_{mn}^p(\omega_{mn}^2 - \omega^2)}. \tag{43}$$

The cross receptances $\beta_{12} = \beta_{21}$ become zero when these solutions are utilized, which is as expected from the reciprocity theorem. Using the same approach in deriving the plate receptances for the single plate–shell case, the plate receptances of a double–shell combination can be systematized as:

(1) The receptance due to the radial displacement response of plate i ($i = 1, 2$) to the tangential loading $F_{ri}(i = 1, 2)$ is

$$\beta_{rr} = \begin{cases} -1/(a\rho h_i\omega^2), & P = 1, \\ 0, & P \neq 1, \end{cases} \tag{44}$$

where $r = 1,3$.

(2) The receptance due to the slope response of plate i ($i = 1, 2$) to the coupling line moment loading $M_{ri}(i = 1, 2)$ is

$$\beta_{ss} = \sum_{m=1}^{\infty} \frac{\pi\lambda_{mn}^2 a[\mathrm{J}_{n+1}(\lambda_{mn}a) - \mathrm{J}_n(\lambda_{mn}a)\mathrm{I}_{n+1}(\lambda_{mn}a)/\mathrm{I}_n(\lambda_{mn}a)]^2}{\rho h_i N_{mn}^p(\omega_{mn}^2 - \omega^2)} \tag{45}$$

where $s = 2, 4$.

The cross receptances $\beta_{12}, \beta_{21}, \beta_{34}, \beta_{43}, \ldots, \beta_{2k-1,2k}$ are all zero from the reciprocity theorem.

4. CURVATURE FACTORS

4.1. BARREL-SHAPED SHELL

If the curvature of a simply supported barrel-shaped shell is not too pronounced, as a rule of thumb in engineering application, $C_s/L_s \leqslant 1/20$ (Figure 1), the transverse mode function of the barrel shell can be approximated by that of the circular cylindrical shell. It satisfies the boundary condition and is of the form

$$U_{3mn}^s(x, \theta) = \sin(m\pi x/L_s)\cos n(\theta - \phi). \tag{46}$$

Also, the natural frequency of the barrel shell is given [30] as

$$\omega_{Bmn}^2 = \omega_{1mn}^2 + \frac{n^2[n^2(a/R)^2 + 2(a/R)(m\pi a/L_s)^2]E}{\rho a^2[(m\pi a/L_s)^2 + n^2]^2}, \tag{47}$$

where ω_{Bmn} is the natural frequency of the barrel-shaped shell with a radius of curvature R, and ω_{1mn} is the natural frequency of the transverse vibration mode of a simply supported cylindrical shell with a radius a, which is given in Appendix A. Replacing the natural frequencies of the cylindrical shell by those of the barrel-shaped shell, the shell receptances formulated in section 3.1 for the cylindrical shell are all applicable to the barrel shell.

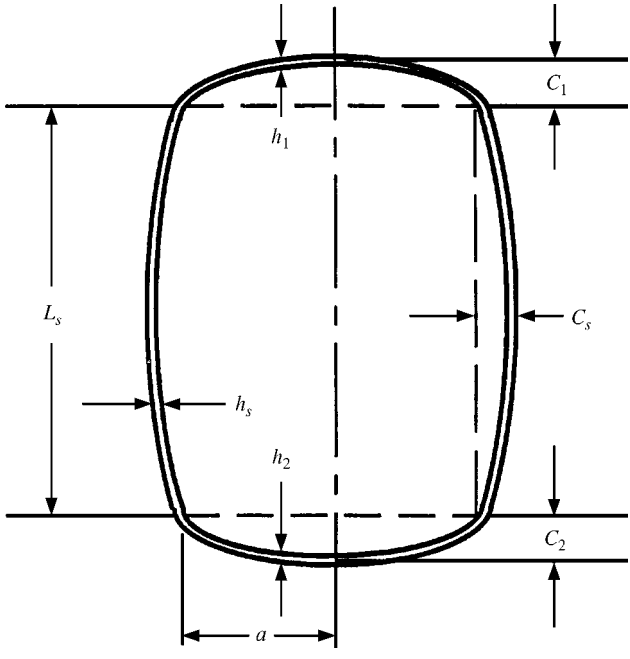

Figure 1. Section view of plate–shell combination consisting of a barrel-shaped shell with two spherically curved plates.

4.2. SPHERICALLY CURVED PLATE

As discussed by Soedel [31], the circular plate with shallow spherical curvature (as a rule of thumb, $C_i/2a \leqslant 1/20$, $i = 1, 2$ (Figure 1)) has the same transverse mode function and the same eigenvalues as those of the flat plate, as long as the boundary conditions are the same. The natural frequency of the spherically curved plate is related to that of the flat plate in the form

$$\omega_{smn}^2 = \omega_{pmn}^2 + \frac{E}{\rho R^2}, \tag{48}$$

where R is the radius of curvature of the curved plate, ω_{smn} is the natural frequency of the spherically curved plate, and ω_{pmn} is the natural frequency of the flat plate, which is given in equation (38). Similarly, replacing the natural frequencies of the flat plate by those of the spherically curved plate, the plate receptances formulated in section 3.2 are all applicable to the curved plate.

5. SOLUTION APPROACH

The Bessel functions (J_n, I_n) used in the formulation of receptances were calculated by IMSL subroutines, so were the eigenvalues (λ_{mn}) of the circular plate. The 4-point Gauss Legendre quadrature numerical integration scheme was implemented to calculate plate modal mass N_{mn}^p in equation (40).

The solutions of the system frequency equation, equation (6), are the natural frequencies of the plate–shell combination. The left-hand side of equation (6) becomes infinite (singular) at each natural frequency of the plate and the shell, with the system frequencies being the

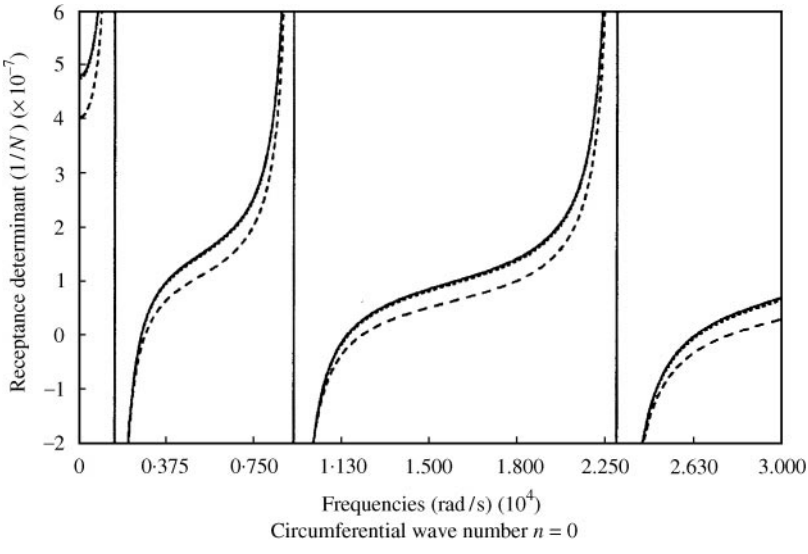

Figure 2. Typical convergence of the left-hand side of equation (6) as a function of the number of terms in series expressions: 10 terms, – – – – –; 30 terms - - - - -; 40 terms, ——.

zeros between the infinities. An iteration method (secant method) was selected to search for these system frequencies. Figure 2 illustrates this since it shows the value of the left-hand side of equation (6) as a function of frequency ω. Zero values correspond to the system natural frequencies. Since all receptances were expressed as series of plate or shell modes, convergence of the solution, as a function of the terms used in the series expressions, was studied. The dashed line in Figure 2 represents series consisting of 10 terms, the dotted line is for 30 terms and the solid line is for 40 terms. In general, it was found that a satisfactory convergence of solutions in the frequency range of interest was achieved using 40 terms.

The individual mode shapes were determined by substituting each system natural frequency back into the displacement equations and calculating the displacement responses due to force and moment loading at each point. The maximum amplitudes of the mode shapes included in this section have been normalized to 15% of the length of the shell for easy viewing. Therefore, they should not be viewed as realistic amplitudes, which would typically not exceed the order of the shell thickness.

6. NUMERICAL RESULTS AND DISCUSSION

Using the receptance approach formulated above, numerical results are presented for three configurations of a plates–shell structure. The shell and the plate are assumed to be made of steel with the material properties: $E = 20{\cdot}6 \times 10^4$ N/mm^2, $\rho = 7{\cdot}85 \times 10^{-9}$ N s^2/mm^4 and $\upsilon = 0{\cdot}3$. The dimensions are $L_s = 200$ mm, $a = 100$ mm, $h_s = 2$ mm and $h_1 = h_2 = 2$ mm, unless stated otherwise.

6.1. CYLINDRICAL SHELL WITH SPHERICALLY CURVED END PLATES (CASE 1)

The natural frequencies and mode shapes of the combined structure (Figure 1), with $D_1 = C_1/a$ and $D_2 = C_2/a$ both equal to 0·1, are computed using the receptance method for

the first four frequencies of each of the lowest six circumferential wave numbers, and shown in Figure 3. Each mode shape is represented by an (M, n) designation, where n is the number of circumferential waves (consider $n = 0$–5 here), and M is the frequency number in ascending order for each n number (consider $M = 1$–4 only). In this case, since the

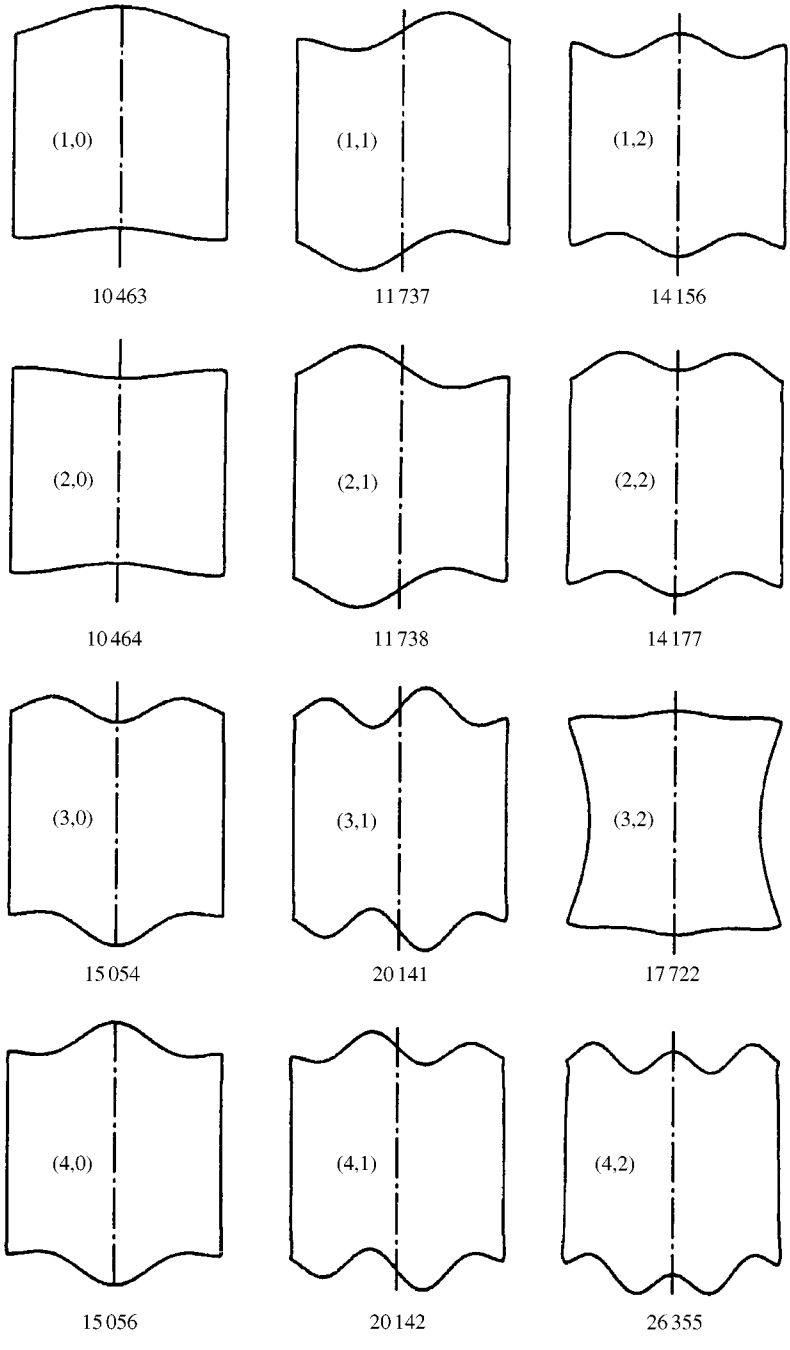

Figure 3. Natural frequencies (rad/s) and mode shapes of a cylindrical shell with spherically curved end plates, $D_1 = D_2 = 0{\cdot}1$ (Case 1). Mode (M, n) is for $M = 1$–4 and $n = 0$–5.

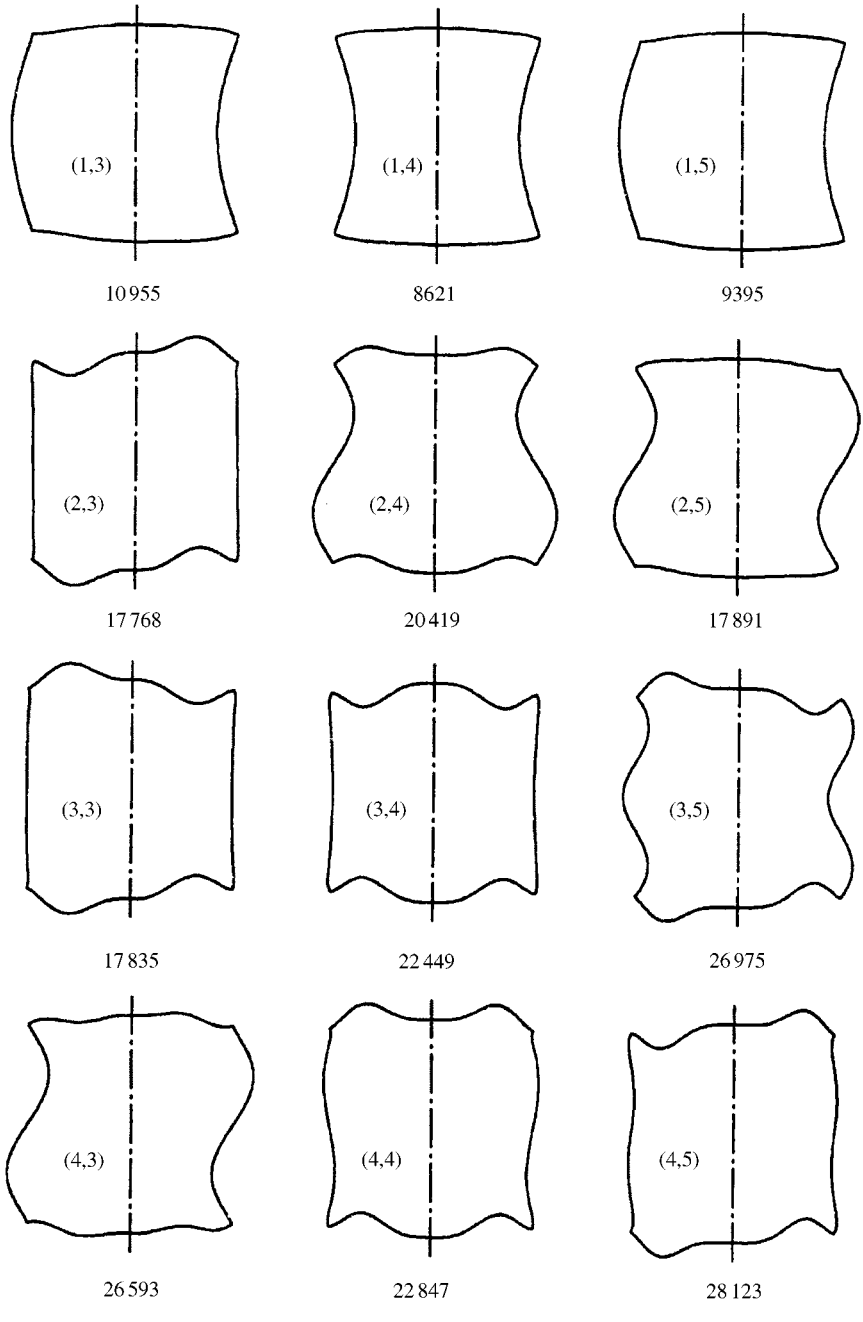

Figure 3. Continued.

plate–shell joints are at the simply supported ends of the shell, the line moment is the only interaction between the plate and the shell. The two subsystems are dynamically coupled to each other only through slope changes. Rigid-body modes of the plate do not come into play in this case, nor is the interaction between the plate and the shell due to a line force. These mode shapes show the normal displacements (transverse deflections) of the spherical

end plates and the radial displacements (transverse deflections) of the shell in cross-section defined by $\theta = 0$ and π.

For the purpose of verifying the results obtained by using the receptance method, the first four natural frequencies and shapes of the $n = 0$ mode type were calculated by using a finite element model [32] with the same geometric characteristics and boundary conditions, and shown in Figure 4. As the analytical results are compared to the numerical results, it is seen that there is, in general, good agreement. However, it is noticed that there are sizable differences between the finite element results and the receptance results as far as the system natural frequencies are concerned. Discrepancies are due to formulations used for the finite element and assumptions made for the system receptances. The membrane effect of the shell is considered to include the in-plane deformation in the formulation of the finite element. However, for simplification, the analytical model does not employ full connection, it assumes that the circular plate is inelastic in its plane and thus neglects possible influences of small connection deflections in the tangential planes of the shell in order to reduce the number of connections of each plate–shell joint. For lower frequencies and modes of the system, the receptance solution based on the formulation of two connections is satisfactory. However, for high frequencies and modes, full connection is necessary.

Figure 5 shows the variation of the natural frequencies with the circumferential wave number ($n = 0$–7) for every lowest frequency in each n family (namely, all $M = 1$ frequencies, from (1, 0), (1, 1), to (1, 7)), of three types of structure. The first is a simply

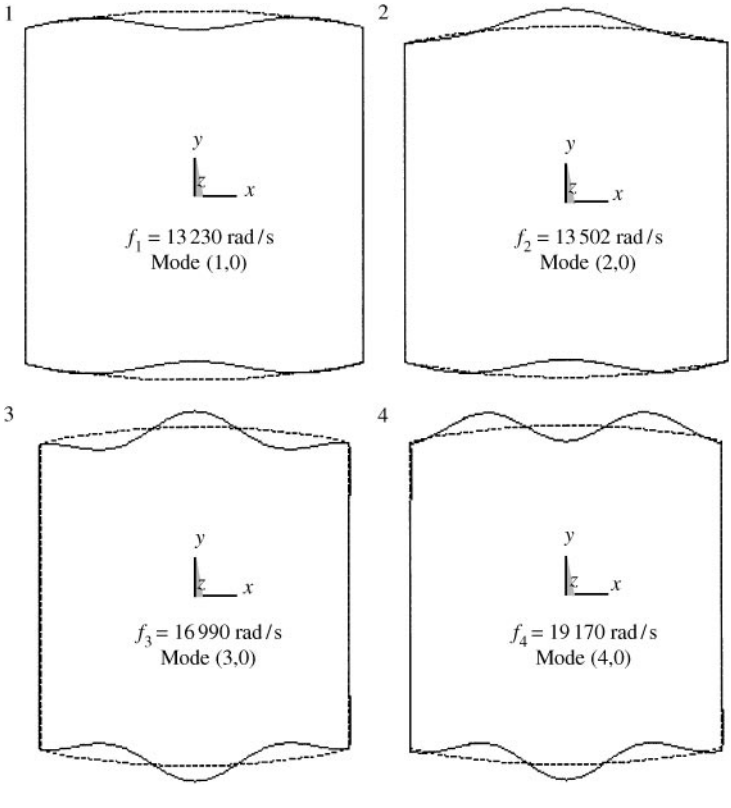

Figure 4. Natural frequencies and mode shapes of a cylindrical shell with spherically curved end plates, $D_1 = D_2 = 0{\cdot}1$ (Case 1), obtained by using the finite element program, ANSYS. They agree with those reported in Figure 3.

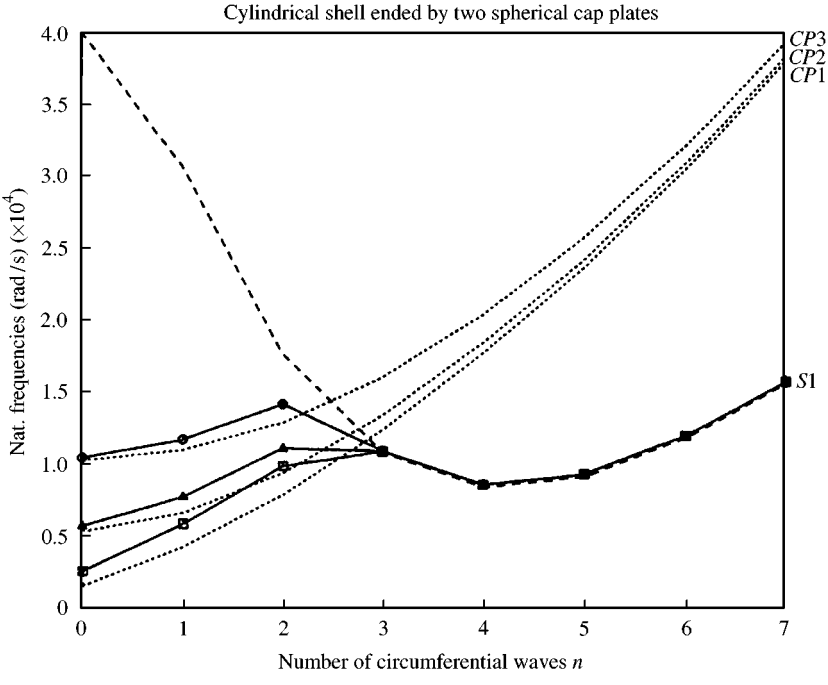

Figure 5. Natural frequencies for Case 1 with three plate configurations ($D_i = 0$, 0·05 and 0·1; $i = 1,2$), plotted as functions of the number of circumferential waves, n, for $M = 1$ (the first frequency for each n) and compared to the natural frequencies of a simply supported plate (·····) with three configurations ($D = 0$, 0·05 and 0·1) and a simply supported cylindrical shell (– – – –). □—□, flat plate; ▲—▲, cap plate A; ○—○, cap plate B.

supported spherically curved plate (in dotted lines, with $D = 0$, 0·05 and 0·1, where $D = C_1/a$ or C_2/a). The second is a simply supported cylindrical shell (in dashed line). The third is a combination of a cylindrical shell and two spherically curved plates (in solid lines) with three plate configuration, namely, both plates flat, both plates curved with $D_1 = D_2 = 0{\cdot}05$, and both plates curved with $D_1 = D_2 = 0{\cdot}1$. It is seen from Figure 5 that, at lower circumferential wave numbers, the natural frequencies of the plate alone (dotted lines) are lower than those of the shell alone (dashed line). Therefore, it is not unexpected that the shell–plate joined structure has plate-controlled vibration characteristics at these numbers. In other words, the plate is mainly responsible for the vibration activity. However, due to the constraining effect of structural coupling with the shell, the natural frequencies of these modes of a joined structure are higher than the natural frequencies of a simply supported curved plate.

It is also seen that in Figure 5, around the area where the plate curves intersect the shell curve, the combined structure happens to exhibit strong coupling between the plate and the shell. It can be viewed as a frequency coincidence between the two uncoupled substructures. As the circumferential wave number becomes larger, the natural frequencies of the shell alone become lower than the natural frequencies of the plate. The natural frequencies of the combined structure are therefore close to those of the shell alone, and the mode shapes of the combined structure are expected to show shell-controlled characteristics with relatively less plate activity.

It is noticed that, in Figure 5, the natural frequencies of the joined structure are raised for modes with lower circumferential wave number as the curvatures of the plates are increased. However, natural frequencies of modes with higher circumferential wave number stay the

same. It explains that the joined structure, with its geometric configuration as described, has plate-controlled vibration modes at lower circumferential wave number ($n = 0$–2). Increasing curvature of the end plate will increase its stiffness, consequently, it will increase the natural frequencies of those plate-controlled modes of the joined structure. However, natural frequencies of the shell-controlled modes, which appear at higher n number ($n = 3$–7), will not be affected by stiffening the end plates by curving them.

In Figure 6, it is seen that, at each of the lower circumferential wave numbers ($n = 0, 1, 2$), the first two natural frequencies ($M = 1, 2$) of the joined structure consisting of a cylindrical shell and two flat plates almost coincide. It is because the thickness and the configurations of the two plates are identical, so the plates have almost the same natural frequencies for these plate-controlled modes. If the curvature of one of the two end plates is increased, from $D = 0$ to 0·1 ($D = C_1/a$ or C_2/a), then the natural frequencies of the $M = 2$ modes will be raised, as shown in Figure 7. The in-phase and the out-of-phase plate-controlled mode pairs, such as modes (1, 0) and (2, 0), (1, 1) and (2, 1) shown in Figure 3, will become more divided. If the curvatures of both end plates are increased to the same amount, the natural frequencies of the lowest two plate-controlled modes of each circumferential wave number ($n = 0$–2) will approach coincidence again, as shown in Figure 8. On reviewing Figures 6–8, it is found that only by introducing asymmetry by increasing the thickness or curvature for one of the two end plates will the natural frequencies of the mode pair appreciably drift apart (mode splitting). The fundamental frequency of the joined structure will not be increased, unless the thickness or curvatures of both the end plates are increased. This is an important practical design concept, for example, in the hermetic compressor industry, where curvatures are introduced to raise the lowest natural frequency of the system for noise control purposes.

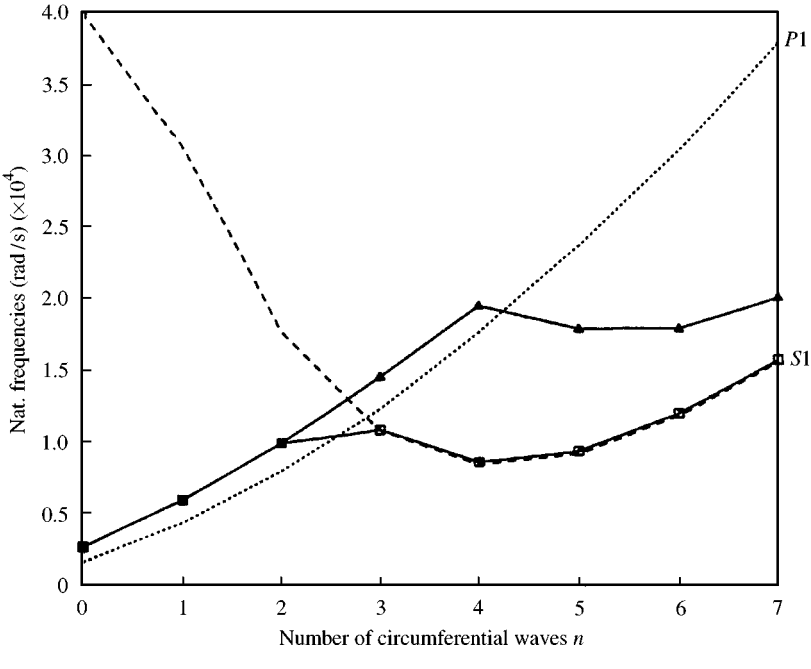

Figure 6. Natural frequencies for Case 1 with two flat end plates ($h_1 = h_2 = 2$ mm and $D_1 = D_2 = 0$), plotted as functions of the circumferential wave number n for $M = 1$ and 2, and compared to the $M = 1$ natural frequencies of a simply supported flat ($D = 0$) circular plate (·····) and a simply supported cylindrical shell (– – – –). □—□, $M = 1$; ▲—▲, $M = 2$.

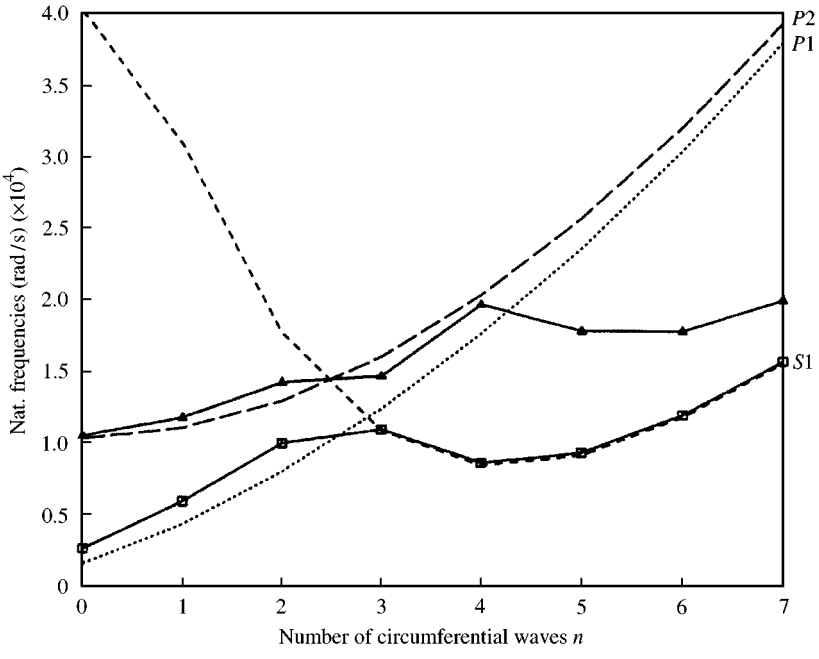

Figure 7. Natural frequencies for Case 1 with two end plates at different curvatures ($h_1 = h_2 = 2$ mm, $D_1 = 0$, $D_2 = 0{\cdot}1$), plotted as functions of the circumferential wave number n for $M = 1$ and 2, and compared to the $M = 1$ natural frequencies of a simply supported curved plate with $D = 0$, (·····), with $D = 0{\cdot}1$, (— —), and a simply supported cylindrical shell (– – – –). □—□, $M = 1$; ▲—▲, $M = 2$.

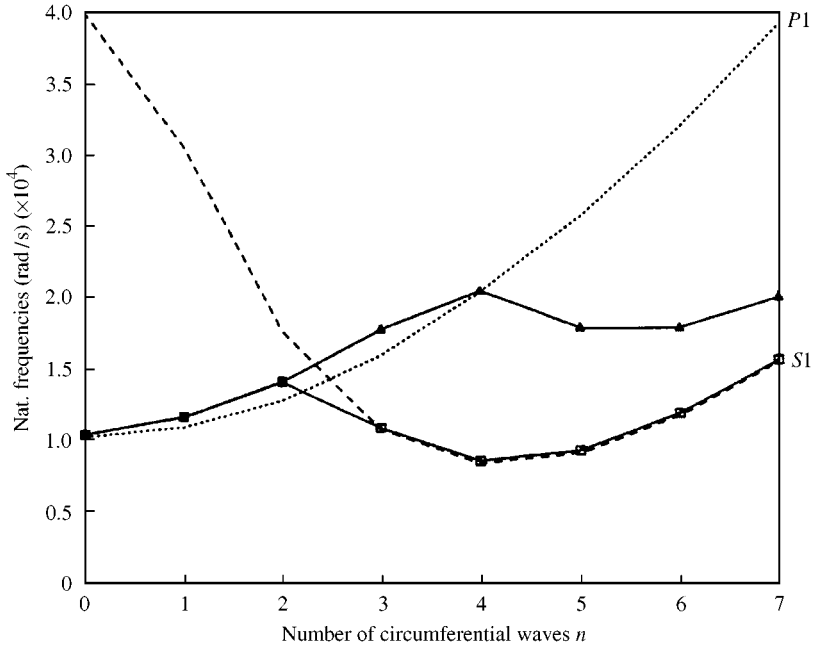

Figure 8. Natural frequencies for Case 1 with two curved end plates ($h_1 = h_2 = 2$ mm, $D_1 = D_2 = 0{\cdot}1$), plotted as functions of the circumferential wave number n for $M = 1$ and 2, and compared to the $M = 1$ natural frequencies of a simply supported curved ($D = 0$) plate (·····) and a simply supported cylindrical shell (– – – –). □—□, $M = 1$; ▲—▲, $M = 2$.

6.2. BARREL-SHAPED SHELL WITH FLAT END PLATES (CASE 2)

The natural frequencies and mode shapes of the flat plate–barrel shell combined structure, with $D_3 = C_s/a = 0{\cdot}1$ (see Figure 1), are computed using the receptance method for the first four frequencies of each of the lowest six circumferential wave numbers ($n = 0$–5), and shown in Figure 9. In order to verify the results obtained by using the receptance method, the first four natural frequencies and shapes of the $n = 0$ mode type

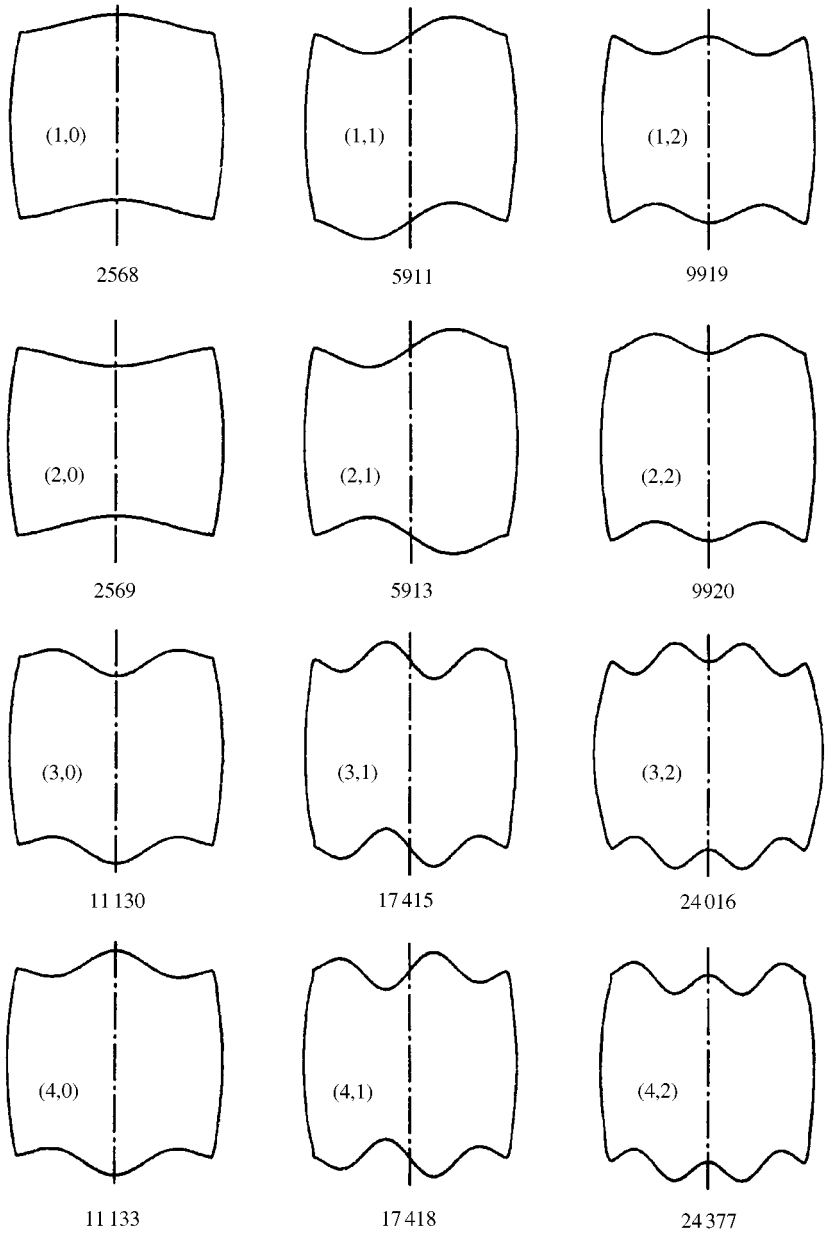

Figure 9. Natural frequencies (rad/s) and mode shapes of a barrel-shaped shell ($D_3 = 0{\cdot}1$) with flat end plates ($h_1 = h_2 = 2$ mm) (Case 2). Mode (M, n) is for $M = 1$–4 and $n = 0$–5.

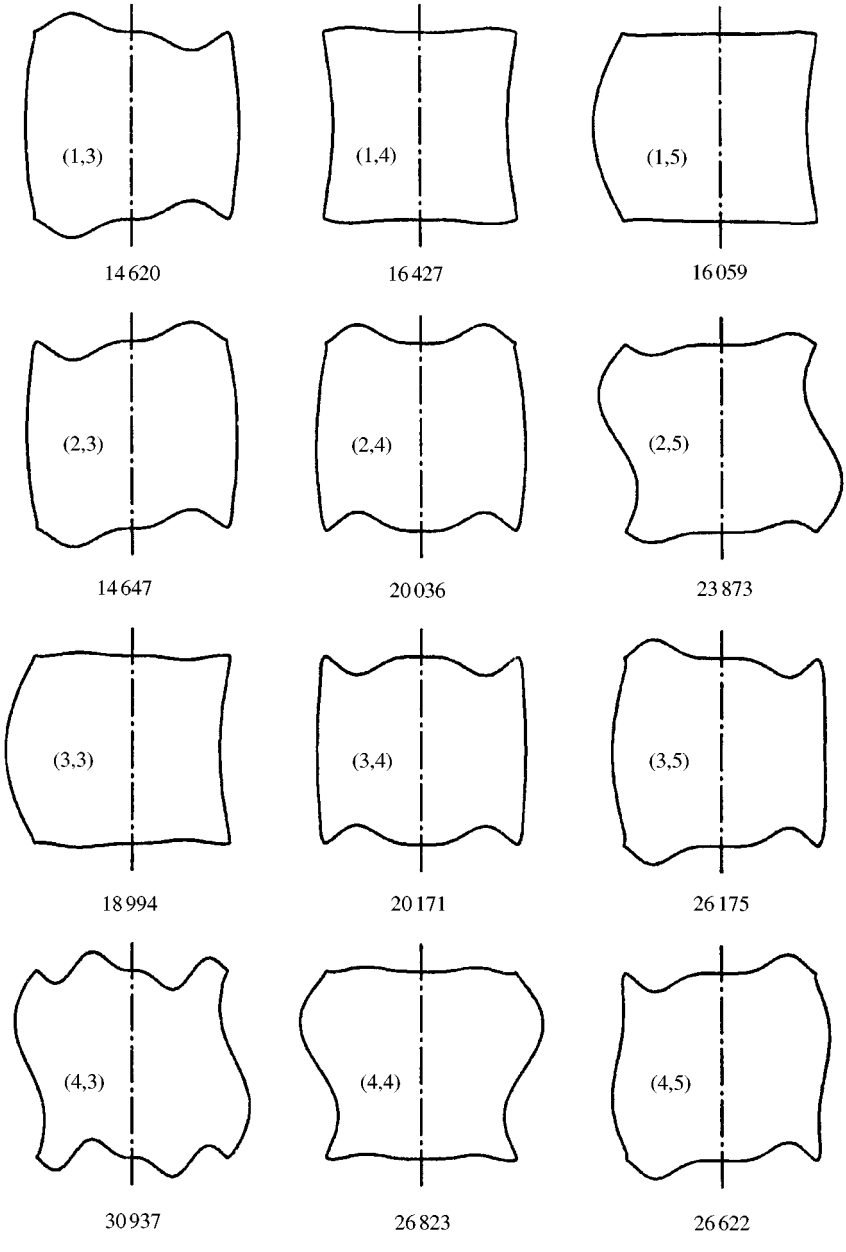

Figure 9. Continued.

were calculated by using a finite element model with the same geometric characteristics and boundary conditions, and shown in Figure 10. Good agreement is found between the analytical results and the numerical results. Therefore, the formulation of the system frequency equation and the solution approach are verified to be correct. On comparison of the corresponding modes of cases 1 and 2, it is found that some modes exhibit dissimilar shapes, such as modes (3, 2), (1, 3), (2, 4) and (3, 5). This resulted from the changes in stiffness of the substructures.

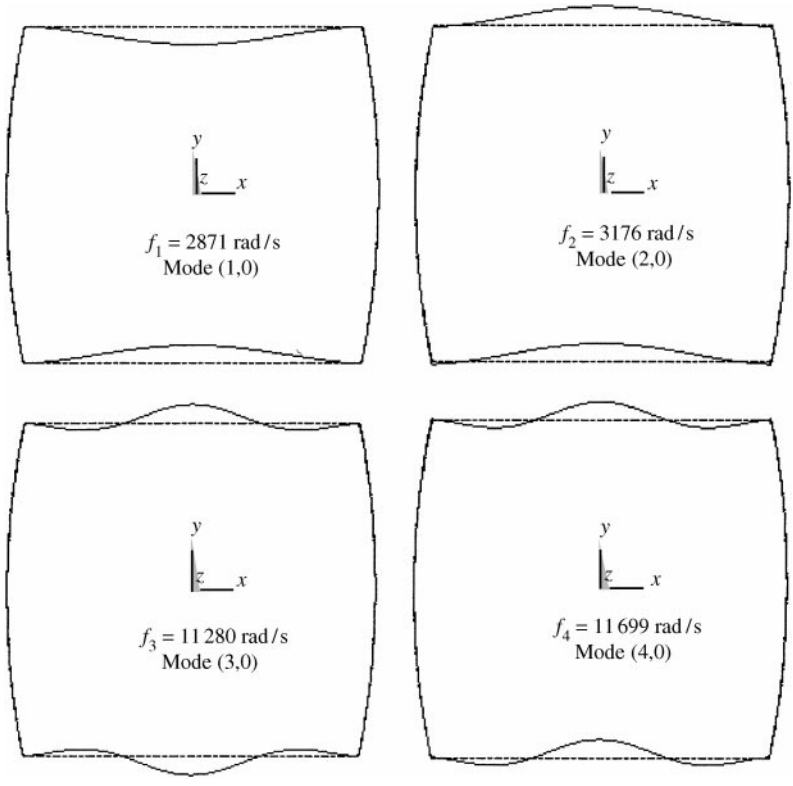

Figure 10. Natural frequencies and mode shapes of a barrel-shaped shell ($D_3 = 0{\cdot}1$) with flat end plates (Case 2) obtained by using the finite element program, ANSYS. They agree with those reported in Figure 9.

Figure 11 shows the variation of the natural frequencies with circumferential wave number ($n = 0$–7) for the lowest frequency ($M = 1$) of three types of structure. The first is a simply supported flat circular plate (dotted line). The second is a simply supported barrel shell (dashed lines), with $D_3 = 0$, 0·05 and 0·1. The third is a combination of a barrel shell and two flat end plates (in solid lines) with three shell configurations, namely, $D_3 = 0$, 0·05 and 0·1. It is noticed that, in Figure 11, the natural frequencies of the joined structure do not change at the lower circumferential wave number ($n = 0$–2) as the curvature of the barrel shell is increased. However, the natural frequencies of modes with higher circumferential wave number ($n = 3$–7) do increase on increase of shell curvature. The explanation is that increasing the shell curvature will increase the modal stiffness and hence increase the natural frequencies of those shell-controlled modes of the joined structure. However, natural frequencies of the plate-dominated modes, which dominate the system in the lower-frequency range, will not be affected by stiffening the shell.

Figure 12 shows the variation of the first three natural frequencies ($M = 1$–3) for each circumferential wave number ($n = 0$–7). It is seen that, at each of the lower circumferential wave numbers ($n = 0$–3), the first two natural frequencies ($M = 1, 2$) of the joined structure consisting of barrel shell and flat end plates coincide. Comparing Figure 12 with Figure 8, it is seen that there are more plate-controlled modes in Figure 12. This can be verified by reviewing the corresponding mode shapes. In Figure 3, modes (1,3) and (1,4) of the joined structure, consisting of a cylindrical shell and spherically curved plates, show shell-dominated behavior, while in Figure 9, modes (1,3) and (1,4) of a barrel shell–flat plate joined structure exhibit stronger plate activity.

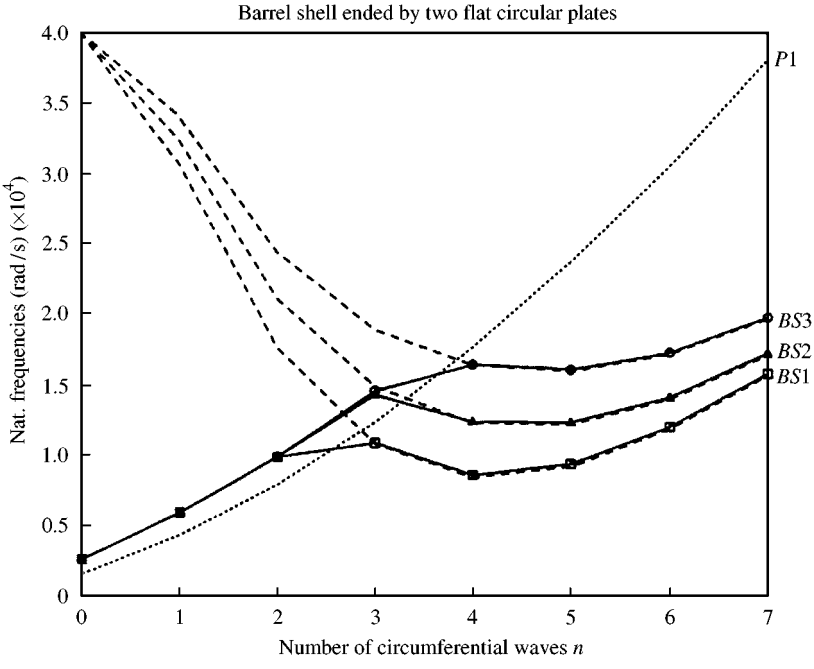

Figure 11. Natural frequencies for Case 2 with three shell configurations ($D_3 = 0$, 0·05 and 0·1), plotted as functions of the circumferential wave number n for $M = 1$, and compared to the natural frequencies of a simply supported flat plate (·····), and a simply supported cylindrical shell (– – – –) with three configurations ($D_3 = 0$, 0·05 and 0·1). □—□, Cylindrical shell; ▲—▲, Barrel shell A; ○—○, Barrel shell B.

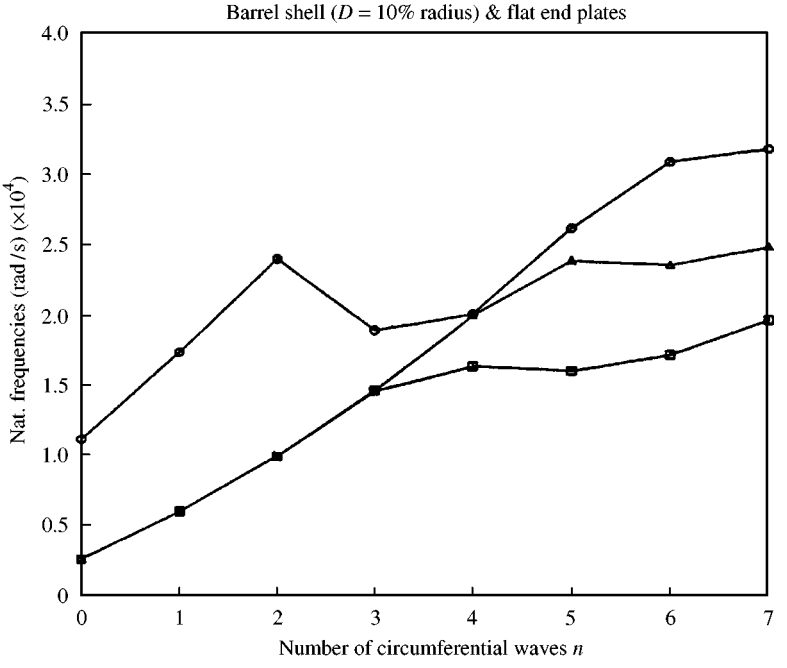

Figure 12. Natural frequencies of a barrel-shaped shell ($D_3 = 0{\cdot}1$) with two flat end plates ($h_1 = h_2 = 2$ mm), plotted as functions of the circumferential wave number n for $M = 1$, 2 and 3. □—□, $M = 1$; ▲—▲, $M = 2$; ○—○, $M = 3$.

6.3. BARREL-SHAPED SHELL WITH SPHERICALLY CURVED END PLATES (CASE 3)

The natural frequencies and modes of the barrel shell–curved plate combined structure, with $D_1 = D_2 = D_3 = 0{\cdot}1$, are computed for the lowest four frequencies of each of the lowest six circumferential wave numbers ($n = 0$–5), and shown in Figure 13. Reviewing mode shapes in these three cases, it is noticed that modes in case 3 resemble those in case 2 more than those in case 1.

Figure 14 shows the variation of the natural frequencies with circumferential wave numbers ($n = 0$–7) for the first frequency ($M = 1$) of three types of structure. The first is

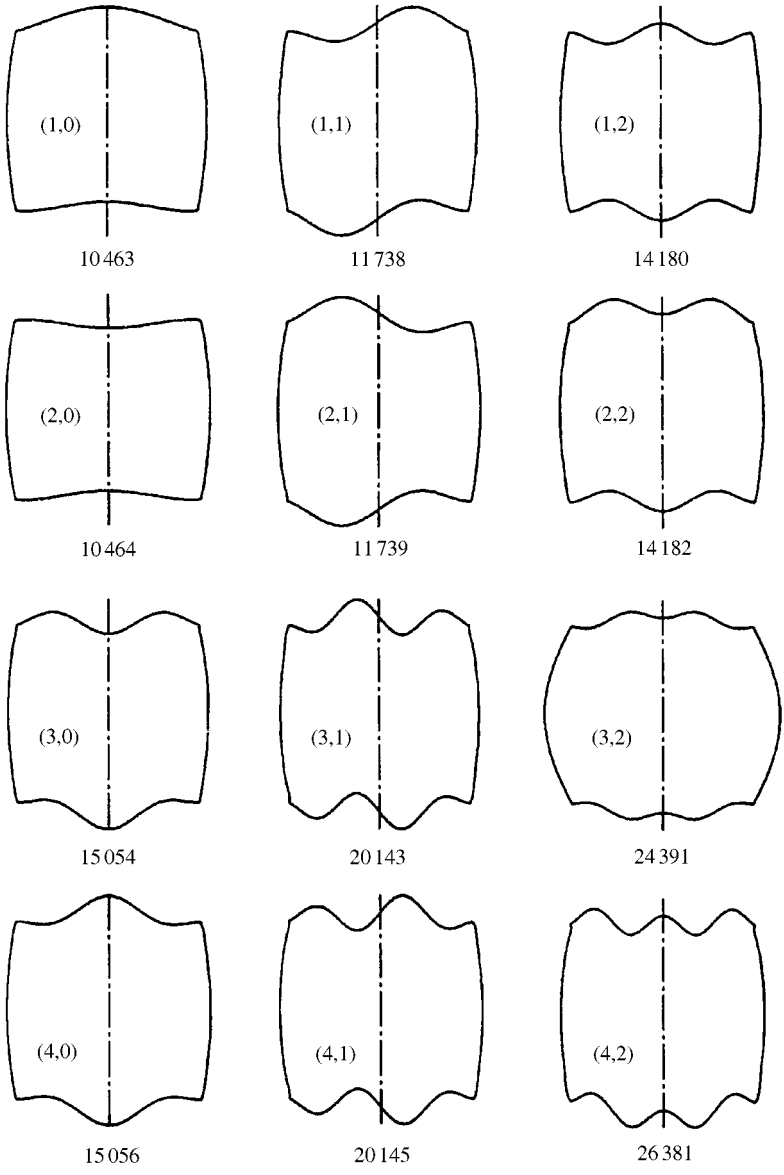

Figure 13. Natural frequencies (rad/s) and mode shapes of a barrel-shaped shell ($D_3 = 0{\cdot}1$) with spherically curved end plates ($D_1 = D_2 = 0{\cdot}1$) (Case 3). Mode (M, n) is for $M = 1$–4 and $n = 0$–5.

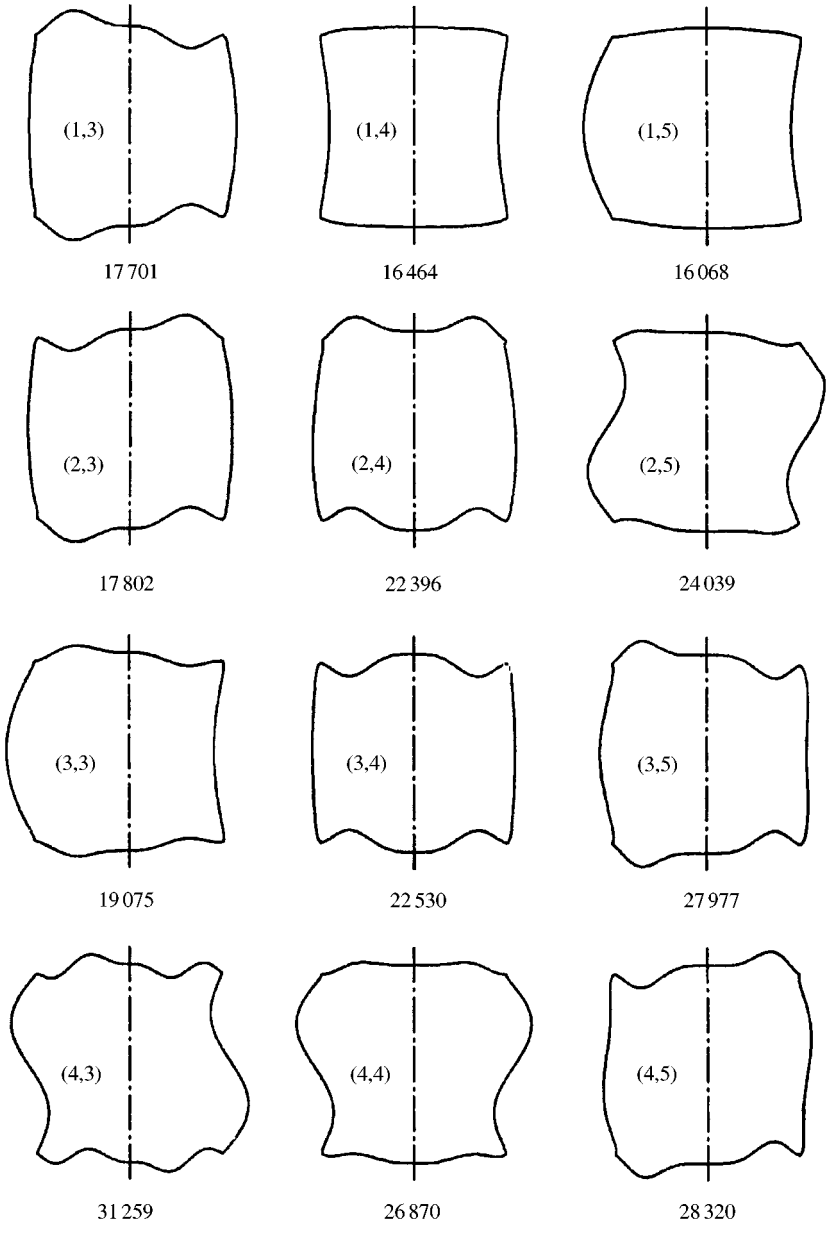

Figure 13. Continued.

a simply supported spherically curved plate (dotted lines) with $D = 0$, 0·05 and 0·1. The second is a simply supported barrel shell (dashed lines) with $D_3 = 0$, 0·05 and 0·1. The third one is a joined structure consisting of a barrel shell and two spherically curved end plates (solid lines) with three configurations of plates and shell, namely, $D_1 = D_2 = D_3 = 0$, 0·05, and 0·1. It is shown in Figure 14 that the natural frequencies of the joined structure increase on increasing the curvatures of the plates and the shell. It indicates that, by making the plate increasingly spherically curved and the shell increasingly barrel-shaped, the modal stiffness of each of the substructures can be increased, and consequently, the natural frequencies of

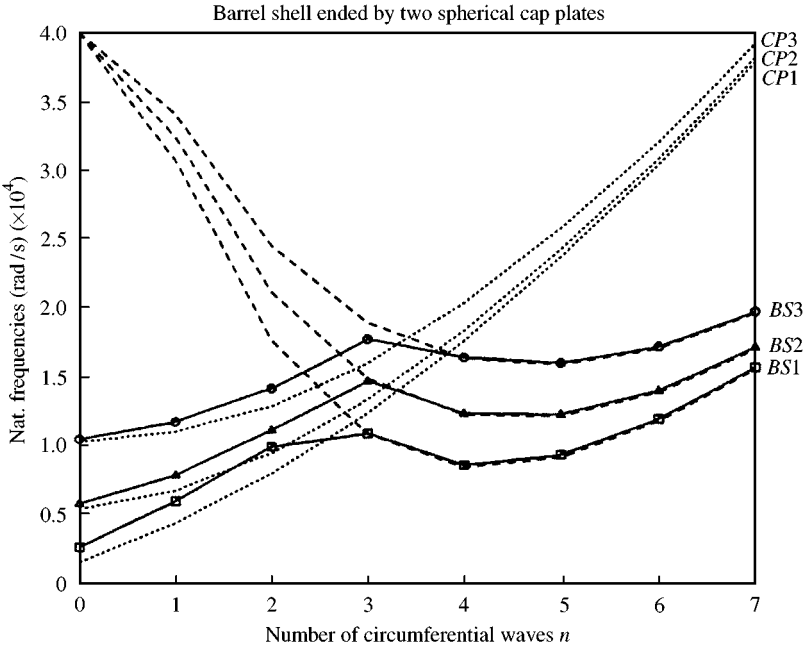

Figure 14. Natural frequencies for Case 3 with three different configurations of the plate and the shell ($D_1 = D_2 = D_3 = 0$, 0·05 and 0·1), plotted as functions of the circumferential wave number n for $M = 1$, and compared to the natural frequencies of a simply supported plate with three configurations ($D = 0$, 0·05 and 0·1), (·····), and a simply supported cylindrical shell with three configurations ($D_3 = 0$, 0·05 and 0·1), (– – – –). □—□, $D = 0\%$; ▲—▲, $D = 5\%$; ○—○, $D = 10\%$.

the joined structure will be increased, not only for the plate-controlled modes, but also for the shell-controlled modes.

7. CONCLUSIONS

This paper is the first one to study the influences of small curvatures on free vibration of a plate–shell combined structure, consisting of a circular barrel-like shell and two spherically curved end plates, using the line receptance concepts and approximate frequency equations of barrel-shaped shell and spherically curved plate. It illustrates in detail the information about the natural frequencies and mode shapes of the combined structure under different geometric configurations. In all cases, it is found that mode pairs can be identified by involving the action of the two plates. Under symmetric conditions, the plate motion will occur in-phase and out-of-phase. If symmetry is eliminated, the mode pair will usually consist of one plate participating strongly in the system mode, with the other's motion suppressed, and vice versa. It is shown that, for plates of the same curvatures, the plate with the minimum thickness will control the lowest system natural frequency. Only when the plates become substantially thicker than the shell, will the shell control the lowest system mode. For plates of the same thickness, it is shown that typically the plate with the minimum curvature will control the lowest system natural frequency.

From the studies reported so far, it is understood that there are at least three ways to detune mode pairs in a multiple plate–shell combined structure. The first way is to connect the plates to the shell at symmetrical axial locations, but to keep the thickness of the plates different. The second way is to keep the thickness of the plates the same, but connect the

plates to the shell at unsymmetrical axial locations. The third one, which this study focuses on, is to keep the thickness the same and the connecting locations symmetrical, but vary the curvatures of the plates.

By either making the plates shallowly curved, or having the shell shallowly barrel-shaped, or both, the corresponding substructures can be stiffened, and consequently, the natural frequencies of the combined structure will be increased. The design rule is that increasing curvature of the plate will increase system natural frequencies in the plate-controlled region, while the system frequencies in the shell-dominated range will not be changed. Conversely, increasing curvature of the shell will increase system frequencies in the shell-dominated range and leave those in the plate-controlled region unchanged. If both the plate and the shell are made to have curved surfaces, then the overall curvature effect will be a superposition of each individual effect.

In order for equations (47) and (48) to be valid, the curvatures of the shell and the plate should not be too pronounced. Very large curvatures, without reducing the base radius, could actually decrease system frequencies since the shell becomes so much larger. However, this study provides, from an analytical point of view, information about how a plate–shell combined structure can be stiffened through introducing small curvatures to each substructure, and the trends of the results agree with practical experiences. It should also be kept in mind that in engineering applications, the curvature may be determined by necessity and not be as restricted as it is in this paper.

REFERENCES

1. B. L. SMITH and E. E. HAFT 1967 *AIAA Journal* **5**, 2080–2082. Vibration of a circular cylindrical shell closed by an elastic plate.
2. B. L. SMITH 1966 *Ph.D. thesis, Kansas State University*. Free vibration of circular cylindrical shells of finite length.
3. Y. HIRANO 1969 *Bulletin of the Japan Society of Mechanical Engineers* **12**, 459–469. Axisymmetric vibrations of thin drums.
4. S. TAKAHASHI and Y. HIRANO 1970 *Bulletin of the Japan Society of Mechanical Engineers* **13**, 240–247. Vibration of a combination of circular plates and cylindrical shells (Report 1, a cylindrical shell with circular plates at ends).
5. S. TAKAHASHI and Y. HIRANO 1971 *Bulletin of the Japan Society of Mechanical Engineers* **14**, 20–28. Vibration of a combination of circular plates and cylindrical shells (Report 2, a cylindrical shell with circular plate in the intermediate section).
6. K. SUZUKI, M. KONNO, T. KOSAWADA and S. TAKAHASHI 1982 *Bulletin of the Japan Society of Mechanical Engineers* **25**, 591–1600. Axisymmetric vibrations of a vessel with variable thickness.
7. K. SUZUKI, S. TAKAHASHI, E. ANZAI and T. KOSAWADA 1983 *Bulletin of the Japan Society of Mechanical Engineers* **26**, 1775–1782. Vibrations of a cylindrical shell with variable thickness capped by a circular plate.
8. T. KOSAWADA, K. SUZUKI and S. TAKAHASHI 1984 *Bulletin of the Japan Society of Mechanical Engineers* **27**, 1983–1989. Vibrations of a combined system of circular plates and a shell of revolution.
9. K. SUZUKI, T. KOSAWADA, T. UEHARA and H. KUMAGAI 1991 *Journal of Sound and Vibration* **144**, 263–279. Free vibrations of a vessel consisting of circular plates and a shell of revolution having varying meridional curvature.
10. T. IRIE, G. YAMADA and Y. MURAMOTO 1984 *Journal of Sound and Vibration* **92**, 107–115. The axisymmetrical response of a circular cylindrical double-shell system with internal damping.
11. T. IRIE, G. YAMADA and Y. MURAMOTO 1984 *Journal of Sound and Vibration* **95**, 31–39. Free vibration of joined conical-cylindrical shells.
12. G. YAMADA, T. IRIE and T. TAMIYA 1986 *Journal of Sound and Vibration* **108**, 297–304. Free vibration of a circular cylindrical double-shell system closed by end plates.
13. M. S. TAVAKOLI and R. SINGH 1989 *Journal of Sound and Vibration* **100**, 97–123. Eigensolutions of joined/hermetic shell structures using the state space method.

14. M. S. TAVAKOLI and R. SINGH 1989 *American Society of Heating, Refrigeration and Air Conditioning Engineers Transactions* **95**, 131–140. State space modeling of refrigeration compressor shell dynamics.
15. M. S. TAVAKOLI and R. SINGH 1990 *Journal of Sound and Vibration* **136**, 141–145. Modal analysis of a hermetic can.
16. L. CHENG and J. NICOLAS 1991 *Journal of Sound and Vibration* **139**, 108–125. Free vibration of a shell–plate system.
17. I. E. SAKAROV 1962 *NASA Technical Translation* **F-341**, 797–805. Use of the method of dynamic rigidity for calculating the frequencies of natural vibrations of build-up shells.
18. L. L. FAULKNER 1969 *Ph.D. Thesis, Purdue University*. Vibration analysis of shell structures using receptances.
19. I. D. WILKEN and W. SOEDEL 1976 *Journal of Sound and Vibration* **44**, 563–576. The receptance method applied to ring-stiffened cylindrical shell: analysis of modal characteristics.
20. I. D. WILKEN and W. SOEDEL 1976 *Journal of Sound and Vibration* **44**, 577–589. Simplified prediction of the modal characteristics or ring-stiffened cylindrical shell.
21. S. AZIMI, J. F. HAMILTON and W. SOEDEL 1984 *Journal of Sound and Vibration* **93,** 9–29. The receptance method applied to the free vibration of continuous rectangular plates.
22. S. AZIMI, W. SOEDEL and J. F. HAMILTON 1986 *Journal of Sound and Vibration* **109**, 79–88. Natural frequencies and modes of cylindrical polygonal ducts using receptance method.
23. S. AZIMI 1988 *Journal of Sound and Vibration* **120**, 19–35. Free vibration of circular plates with elastic edges supports using the receptance method.
24. S. AZIMI *Journal of Sound and Vibration* **120**, 37–52. Free vibration of circular plates with elastic or rigid interior support.
25. D. T. HUANG and W. SOEDEL 1993 *Journal of Sound and Vibration* **162**, 403–427. Natural frequencies and modes of a circular plate welded to a circular cylindrical shell at arbitrary axial positions.
26. D. T. HUANG and W. SOEDEL 1993 *Journal of Sound and Vibration* **166**, 315–339. On the free vibration of multiple plates welded to a cylindrical shell with special attention to mode pairs.
27. D. T. HUANG and W. SOEDEL 1993 *Journal of Sound and Vibration* **166**, 341–369. Study of the forced vibration of shell-plate combinations using the receptance method.
28. S. K. WONG and K. Y. SZE 1998 *Journal of Sound and Vibration* **209**, 593–607. Application of matched asymptotic expansions to the free vibration of a hermetic shell.
29. R. E. D. BISHOP and D. C. JOHNSON 1960 *The Mechanics of Vibration*. London: Cambridge University Press.
30. W. SOEDEL 1981 *Vibrations of Shells and Plates*. New York: Marcel Dekker.
31. W. SOEDEL 1973 *Journal of Sound and Vibration* **29**, 457–461. A natural frequency analogy between spherically curved panels and flat plates.
32. *ANSYS User's Manual*, Revision 5.6, Houston, PA, USA: 1999. Swanson Analysis System Inc.

APPENDIX A: EQUATIONS OF NATURAL FREQUENCIES AND MODES OF A SIMPLY SUPPORTED CYLINDRICAL SHELL [30]

The natural frequencies of the transverse mode are given as

$$\omega_{1mn}^2 = -\tfrac{2}{3}\sqrt{a_1^2 - 3a_2}\cos(\alpha/3) - a_1/3.$$

The natural frequencies of the longitudinal mode are given as

$$\omega_{2mn}^2 = -\tfrac{2}{3}\sqrt{a_1^2 - 3a_2}\cos\left(\frac{\alpha + 2\pi}{3}\right) - \frac{a_1}{3},$$

The natural frequencies of the circumferential mode are given as

$$\omega_{3mn}^2 = -\tfrac{2}{3}\sqrt{a_1^2 - 3a_2}\cos\left(\frac{\alpha + 4\pi}{3}\right) - \frac{a_1}{3},$$

where

$$\alpha = \cos^{-1}\left(\frac{27a_3 + 2a_1^3 - 9a_1a_2}{2\sqrt{(a_1^2 - 3a_2)^3}}\right),$$

$$a_1 = -\frac{1}{\rho h}(k_{11} + k_{22} + k_{33}),$$

$$a_2 = -\frac{1}{(\rho h)^2}(k_{11}k_{33} + k_{22}k_{33} + k_{11}k_{22} - k_{23}^2 - k_{12}^2 - k_{13}^2),$$

$$a_3 = -\frac{1}{(\rho h)^3}(k_{11}k_{23}^2 + k_{22}k_{13}^2 + k_{33}k_{12}^2 + 2k_{12}k_{23}k_{13} - k_{11}k_{22}k_{33}),$$

where

$$k_{11} = K\left[\left(\frac{m\pi}{L}\right)^2 + \frac{1-\mu}{2}\left(\frac{n}{a}\right)^2\right],$$

$$k_{12} = k_{21} = K\left(\frac{1+\mu}{2}\right)\left(\frac{m\pi}{L}\right)\left(\frac{n}{a}\right),$$

$$k_{13} = k_{31} = \frac{\mu K}{a}\left(\frac{m\pi}{L}\right),$$

$$k_{22} = \left(K + \frac{D}{a^2}\right)\left[\frac{1-\mu}{2}\left(\frac{m\pi}{L}\right)^2 + \left(\frac{n}{a}\right)^2\right],$$

$$k_{23} = k_{32} = -\frac{Kn}{a^2} - \frac{Dn}{a^2}\left[\left(\frac{m\pi}{L}\right)^2 + \left(\frac{n}{a}\right)^2\right],$$

$$k_{33} = D\left[\left(\frac{m\pi}{L}\right)^2 + \left(\frac{n}{a}\right)^2\right]^2 + \frac{K}{a^2}.$$

The mode amplitude ratios (A_{kmn}/C_{kmn}) and (B_{kmn}/C_{kmn}), $k = 1, 2, 3$, are

$$A_{kmn}/C_{kmn} = -\frac{k_{13}(\rho h\omega_{kmn}^2 - k_{22}) - k_{12}k_{23}}{(\rho h\omega_{kmn}^2 - k_{11})(\rho h\omega_{kmn}^2 - k_{22}) - k_{12}^2},$$

$$B_{kmn}/C_{kmn} = -\frac{k_{23}(\rho h\omega_{kmn}^2 - k_{11}) - k_{21}k_{13}}{(\rho h\omega_{kmn}^2 - k_{11})(\rho h\omega_{kmn}^2 - k_{22}) - k_{12}^2}.$$